RESEARCH ARTICLE

Synthesis and characterization of peptide conjugated human serum albumin nanoparticles for targeted cardiac uptake and drug delivery

Nikita Lomis[1,2], Susan Westfall[3], Dominique Shum-Tim[4], Satya Prakash[1,2]*

1 Biomedical Technology and Cell Therapy Research Laboratory, Department of Biomedical Engineering, Montreal, QC, Canada, 2 Division of Experimental Medicine, Montréal, QC, Canada, 3 Meakins Christie Laboratories, Department of Microbiology and Immunology, McGill University, Montréal, QC, Canada, 4 Division of Cardiac Surgery and Surgical Research, Royal Victoria Hospital, Montréal, QC, Canada

* satya.prakash@mcgill.ca

Abstract

Congestive heart failure, a prominent cardiovascular disease results primarily from myocardial infarction or ischemia. Milrinone (MRN), a widely used clinical drug for heart failure, improves myocardial contractility and cardiac function through its inotropic and vasodilatory effects. However, lacking target specificity, it exhibits low bioavailability and lower body retention time. Therefore, in this study, angiotensin II (AT1) peptide conjugated human serum albumin nanoparticles (AT1-HSA-MRN-NPs) have been synthesized for targeted delivery of MRN to the myocardium, overexpressing AT1 receptors under heart failure. The NPs were surface functionalized through a covalent conjugation reaction between HSA and AT1. Nanoparticle size was 215.2±4.7 nm and zeta potential -28.8±2.7 mV and cumulative release of MRN was ~72% over 24 hrs. The intracellular uptake of nanoparticles and cell viability was studied in H9c2 cells treated with AT1-MRN-HSA-NPs vs the control non-targeted drug, MRN Lactate under normal, hypoxic and hypertrophic conditions. The uptake of AT1-HSA-MRN-NPs in H9c2 cells was significantly higher as compared to non-targeted nanoparticles, and the viability of H9c2 cells treated with AT1-MRN-HSA-NPs vs MRN Lactate was 73.4±1.4% vs 44.9±1.4%, respectively. Therefore, AT1-HSA-MRN-NPs are safe for *in vivo* use and exhibit superior targeting and drug delivery characteristics for treatment of heart failure.

Introduction

Cardiovascular disease (CVD) is one of the leading causes of mortality, with incidences constantly on the rise across the developed and developing world. Of these CVDs, myocardial infarction (MI) and congestive heart failure (CHF) are responsible for more than 50% of the global cases of CVDs with high rates of readmission and re-hospitalization [1]. Currently, the most common treatments for CHF include surgical interventions such as heart transplant,

stenting, bypass surgeries, ventricular assist devices and medical treatments including drugs such as Angiotensin Converting Enzyme (ACE) inhibitors, beta blockers, vasodilators etc. [2, 3]. However, despite these common treatment modalities, the average survival rate for more than 50% of patients who have suffered a first heart failure is less than 5 years [4]. Therefore, there is an urgent need for development of effective therapies to target these diseases.

CHF is typically caused by blockage of the coronary artery, which results in ischemia and leads to an irreversible necrosis of the cardiomyocytes. It is widely suggested that under MI and CHF, an overexpression of the angiotensin II type 1 receptors (AT1Rs) on the myocardium may be an underlying cause for cardiac remodeling [5–8]. This facilitates the underlying mechanism of ACE inhibitor drugs, which block the overexpressed AT1 receptors to prevent cardiac hypertrophy [9, 10]. The condition of overexpression of AT1Rs has been explored by a study in which superior AT1R targeting was reportedly achieved for delivery of AT1 bound quantum dot nanoparticles [11]. The use of AT1-conjugated liposomes in a mouse model of MI has also shown their specific internalization [5]. This will be the first study demonstrating a new synthesis scheme for development of a novel nanoparticle formulation, AT1-H-SA-MRN-NPs, for targeted drug delivery to the heart.

Previously, we presented the preparation and binding of HSA-NPs with milrinone (MRN), a cardiac inotrope and vasodilator drug, widely used for the treatment of CHF [12]. Milrinone is a phosphodiesterase III enzyme inhibitor which increases the intracellular cAMP concentration, providing higher calcium influx to create a positive inotropic effect [13–15]. Clinically administered as a lactate formulation (MRN Lactate), milrinone is known to improve the overall cardiac function by increasing myocardial contractility and decreases systemic vascular resistance [16, 17]. However, the lack of target specificity, lower bioavailability and a half-life of approximately 1–2 hours in humans, necessitates its use as a continuous infusion, also causing other side effects such as renal dysfunction, palpitations and arrhythmias [18, 19].

The enhanced targeting and delivery of MRN could be achieved by loading it on nanoparticles targeted to the intended site of action. One of the most widely used nanoparticles are HSA-NPs owing to unique features like biocompatibility, biodegradability and non-immunogenicity. The HSA molecule possesses multiple pockets to promote binding of various hydrophilic and hydrophobic drugs such as paclitaxel, doxorubicin etc. [20–22]. Computational modeling and enzyme release studies have shown that MRN binds hydrophobically to the HSA molecule [12, 23]. HSA-NPs are known to improve the blood circulation time of otherwise insoluble or free drugs and are anticipated to improve the bioavailability of MRN as well [24, 25].

The presence of active functional groups on HSA allows opportunities for surface-modification to bind additional ligands such as peptides, antibodies, genes, and other molecules [26–29]. This would be useful in enhancing receptor mediated nanoparticle internalization and drug delivery characteristics. In this study, HSA was surface modified through a two-step reaction scheme to bind the AT1 peptide to form AT1-HSA. The AT1-HSA was further bound to the cardiac inotrope and vasodilator drug, MRN, to form AT1-HSA-MRN-NPs. In addition to studying drug binding and release, cell viability analysis was performed to compare the safety of AT1-HSA-MRN-NPs with MRN Lactate, which is the clinical drug formulation for CHF treatment. These studies indicate that the novel AT1-HSA-MRN-NPs can bind and deliver MRN and must be tested *in vivo* for use in cardiovascular diseases.

Materials and methods

Materials

Human serum albumin (> 97% lyophilized) was purchased from Sigma Aldrich (Oakville, ON, Canada). Glutaraldehyde (25% aq. solution) was purchased from Alfa Aesar (Cedarlane,

Burlington, ON, Canada). Fluorescein isothiocynate human serum albumin (FITC-HSA) was purchased from Sigma Aldrich (Oakville, ON, Canada). Milrinone was purchased from Selleck Chemicals (Burlington, ON, Canada). Bradford reagent was purchased from Bio-Rad (St. Laurent, QC, Canada). The 5(6)-Carboxyfluorescein N-hydroxysuccinimide was purchased from Thermo Fisher Scientific (ON, Canada) Other chemicals were purchased from Fisher Scientific (Nepean, ON, Canada).

Synthesis of AT1-peptide

The Angiotensin II Type 1 (AT1) receptor targeting peptide is a chain of 8 amino acids Asp-Arg-Val-Tyr-Ile-His-Pro-Phe, and was synthesized by CanPeptide (Pointe-Claire, QC, Canada) as NH_2-Gly-Gly-Gly-Gly-Asp-Arg-Val-Tyr-Ile-His-Pro-Phe-NH_2 along with a Scrambled Peptide NH_2- Gly-Gly-Gly-Gly-Phe-His-Tyr-Arg-Asp-Val-Ile-Pro-NH_2 following the sequence mentioned by Dvir et al. [5].

Surface modification of HSA with AT1 peptide

The surface of HSA was modified to facilitate attachment of the AT1 peptide in a two-step reaction. An aqueous solution of 20 mg/mL of HSA dissolved in deionized water (0.3 mM) was prepared and reacted with a 10-fold molar excess of 5(6)-Carboxyfluorescein N-hydroxy-succinimide ester (COOH-FITC-NHS)), for 1 hour. This was further reacted with EDC/Sufo-NHS for 30 minutes followed by reaction with either the AT1 or scrambled peptide (Scr) for 4 hours (Fig 1). The AT1 and Scr peptide was added in a 10-fold molar excess than HSA. The AT1-HSA and Scr-HSA were purified by dialysis using the Slide-a-Lyze dialysis cassette (10,000 Da MWCO). The purified sample was then lyophilized and stored at 4˚C.

Nuclear magnetic resonance

1D proton spectra were recorded at 25˚ on a 500 MHz Varian INOVA NMR Spectrometer, with an HCN triple resonance RT probe with Z-axis pulsed field gradients. Spectra were
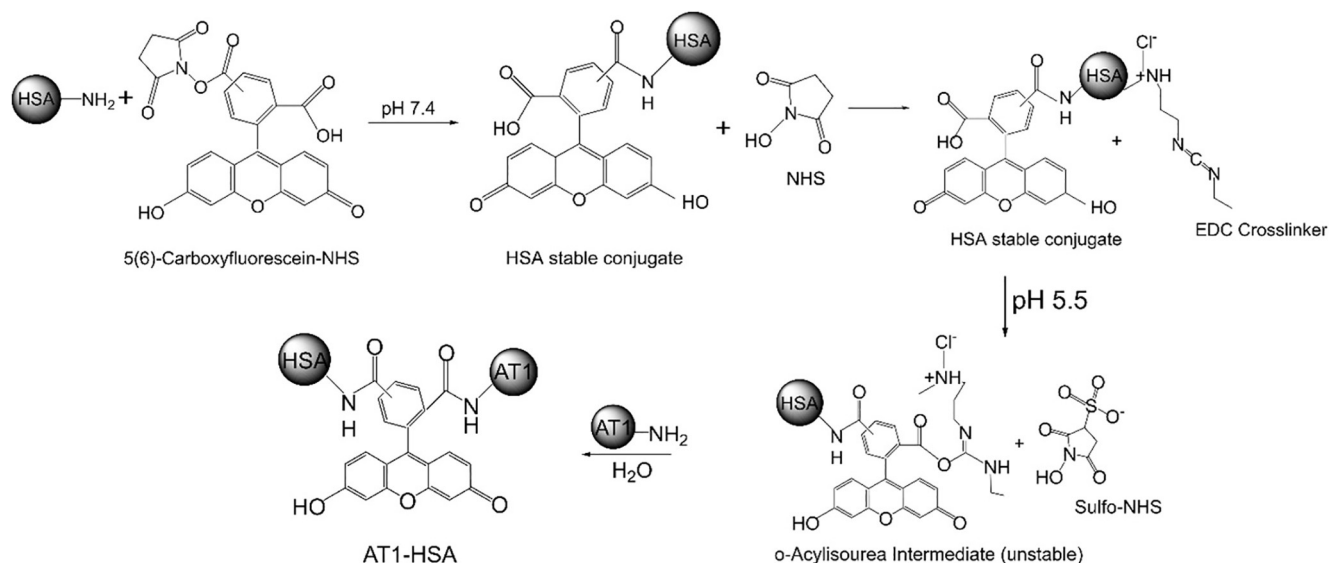
Fig 1. HSA surface modification. Schematic representation of AT1 peptide conjugation to HSA surface through a two-step chemical covalent reaction using fluorescent heterobifunctional cross-linkers.

recorded with double pulsed-field gradient spin echo for suppression of residual H_2O signal. 256 scans with a recycle delay of 1s were collected with a sweep width of 8000 Hz and an acquisition time of 1s. Data were processed with 1 Hz line broadening using the VNMRJ 4.2 software. The concentrations of HSA, AT1 peptide and AT1-HSA were 5 mg/mL in D_2O.

Mass spectrometry

The AT1-HSA, HSA and AT1 peptide samples were analyzed by the Matrix-Assisted Laser Desorption/Ionization Time of Flight Mass Spectrometry (MALDI-TOF-MS) MALDI Auto-flex III- TOF-(BRUKER) SMARTBEAM) (Dept. of Chemistry, McGill University, Montreal, QC, Canada) in linear positive mode. Dihydroxybenzoic Acid was used as the Matrix and the AT1-HSA, HSA and AT1 peptide samples were dissolved in water at concentrations of approximately 7 mg/mL.

Nanoparticle preparation

The AT1-HSA-MRN-NPs were prepared by following the ethanol desolvation technique [30, 31]. Briefly, an aqueous solution of 20 mg/mL of AT1-HSA was prepared in deionized water. The pH of the solution was adjusted to pH 8.0 using 0.1 M NaOH. MRN was dissolved in DMSO and added to the AT1-HSA solution with a final MRN/HSA ratio of 1:20 by weight. Ethanol was added in a dropwise manner resulting in solution turbidity. Glutaraldehyde (8% v/v aq. solution) was added to the reaction mixture at a concentration of 0.588 μl/mg HSA and polymerized for 24 hours. AT1-HSA was substituted with Scr-HSA for preparation of Scr-HSA-NPs and with FITC-HSA for preparation of FITC-HSA-MRN-NPs. The nanoparticles were washed by three rounds of ultracentrifugation at 16500 rpm for 15 minutes each at 25˚C. Supernatant was collected for detection of unbound MRN. The pellet was washed with deionized water and finally re-dispersed in phosphate buffer saline (PBS). The nanoparticles were tip-sonicated for 10 minutes and stored at 4˚C.

Nanoparticle characterization, yield and encapsulation efficiency

The average particle size of the nanoparticles was measured by Dynamic Light Scattering (DLS) using a Particle Size Analyzer (Brookhavens Instruments Corporation, NY, USA). The samples were diluted 1:20 with deionized water and measured at a scattering angle of 90˚ and temperature of 25 ˚C. The Polydispersity Index (PDI) estimated the size distribution of the nanoparticles. The zeta potential was measured by a Zeta Potential Analyzer (Brookhavens Instruments Corporation, NY, USA) using electrophoretic laser Doppler anemometry. The size and shape of the nanoparticles were examined by Transmission Electron Microscopy (TEM) (FEI Tecnai G^2 Spirit Twin 120 kV Cryo-TEM, Gatan Ultrascan 4000 4k x 4k CCD Camera System Model 895).

The yield of the nanoparticles was measured by the UV-spectrophotometric method. A standard curve of HSA solution dissolved in Bradford reagent was used as a reference and absorbance was measured at 595 nm. To determine encapsulation efficiency, nanoparticles were spin concentrated using centrifugal filters with molecular weight cut off (MWCO) of 10,000 Da for eluting the non-encapsulated MRN into the collection tube. A standard curve of MRN in a mixture containing DDQ/Ethanol was used as a reference and absorbance was measured at 356 nm [32].

In Vitro milrinone release from nanoparticles

The *in vitro* drug release was studied by UV-visible spectrophotometry [9]. In brief, 40 mg of AT1-HSA-MRN-NPs were suspended in 10 mL of PBS at 37˚C and 120 rpm in a shaking

incubator. At predetermined time intervals of 0, 0.25, 0.5, 0.75, 1, 2, 4, 8, 18 and 24 hours, 0.5 mL of the nanoparticle suspension was withdrawn and re-substituted with 0.5 mL of fresh PBS. The withdrawn suspension was centrifuged using Amicon centrifugal filters (10K MWCO) and supernatant was used to determine the amount of MRN released. The MRN was detected at 356 nm using a colorimetric assay and a cumulative MRN release over time was calculated [21].

Cell culture and viability

Rat cardiomyoblasts (H9c2) cells were received as a kind gift from Dr. Renzo Cecere, M.D. (Montreal General Hospital, QC, Canada). The H9c2 cells were grown in Dulbecco's Modified Eagle Medium (DMEM) supplemented with 10% fetal bovine serum (FBS). H9c2 cells were seeded at an initial density of 5000 cells/well in clear bottom 96-well black plates for 24 hours in a humidified incubator at 37°C and 5% CO_2, Cells were treated with AT1- HSA-MRN-NPs, AT1-HSA-NPs, MRN-HSA-NPs and MRN Lactate, diluted in serum-free cell culture medium. The MRN concentration in the nanoparticles and MRN Lactate were 1 mM, as optimized from previous studies [12]. After 4, 24 and 48 hours of incubation, the cells were washed thrice with PBS. Cells were treated with 100 μL of fresh cell culture medium and 20 μL of MTT reagent and incubated at 37°C and 5% CO_2 for 4 hours. The media was removed, and cells were lysed by addition of 100 μL of DMSO for 15 minutes at room temperature. The absorbance was measured at 570 nm using the Victor3V 1420 Multilabel Counter spectrophotometer.

Overexpression of the AT1 Receptor

The H9c2 cells were seeded at an initial density of 5,000 cell/well in 96-well plates, separated into three groups: Normal, Hypoxic and Hypertrophic. Hypoxia was induced by treatment with 100 μM of $CoCl_2.6H_2O$ for 24 hours, which simulated the conditions of MI [33]. Hypertrophy was induced by treatment with 20 μM H_2O_2 for 48 hours to simulate conditions of CHF [34]. The cells in each group were treated with the anti-AT1 antibody (Abcam, Canada) for 1 hour followed by a goat polyclonal secondary antibody conjugatedto Alexa 488 (Abcam, Canada) for an additional 1 hour, following the manufacturer's recommended dilutions. The cells were fixed with 4% paraformaldehyde in PBS for 10 mins and thrice washed with PBS and stored at 4°C. The fluorescence was measured at 495 nm excitation/ 519 nm emission wavelengths.

Intracellular nanoparticle uptake

The H9c2 cells were seeded at an initial density of 5,000 cell/well in 96-well plates, separated into three groups: Normal, Hypoxic and Hypertrophic. Cells were subjected to hypoxia by treatment with 100 μM of $CoCl_2.6H_2O$ for 24 hours, to simulated MI [33]. Cells were subjected to hypertrophy by treatment with 20 μM H_2O_2 for 48 hours to simulate HF [34]. The H9c2 cells in each group were treated with 0.5 mg/mL of fluorescently tagged AT1-HSA-MRN-NPs, Scr-HSA-MRN-NPs and MRN-HSA-NPs for 4 hours. The Scr peptide was the same amino acid chain as AT1 peptide but in a scrambled order [20]. The Scr peptide-tagged NPs were used to confirm the targeting efficiency of the AT1 peptide-tagged NPs. The cells were washed thrice with PBS and fresh media was added. The fluorescence intensity was measured at 489nm/535nm using a Victor3V 1420 Multilabel Counter spectrophotometer (Perkin Elmer, Woodbridge, ON, Canada).

Statistical analysis

All statistical analyses were carried out using the GraphPad Prism (v 8.4.3; GraphPad Software, La Jolla, CA) software. One-Way ANOVA with Tukey's multiple comparisons was used to compare the means. All data are expressed as mean ± standard deviation (SD) with n = 3.

Results

Nuclear magnetic resonance

The design and synthesis of the AT1-HSA was initially characterized by ^{1}H-NMR (**Fig 2**). The NMR spectrum of AT1 displays peaks at around 6.8 ppm which are due to the presence of tyrosine residues, while most of the downfield resonance is due to histidine. This signal is also visible on the AT1-HSA spectrum. The spectrum contains two sets of signals. The more intense signals arise from the trans peptide bonds whereas the less intense signals are due to a cis-bond between proline and histidine [21]. Peaks at around 4.0 ppm due to glycine residues visible on AT1 spectrum is also visible on the AT1-HSA spectrum. However, the NMR spectra of the HSA-AT1 and HSA in comparison to AT1 peptide displayed broader peaks, which results from the higher molecular weight (66500 Da) of the HSA in comparison with the AT1 peptide (1274 Da). Thus, the data gathered from ^{1}H-NMR indicate the conjugation of the AT1 peptide with the HSA, which was also confirmed with Mass Spectrometry.

Mass spectrometry

To validate the conjugation of AT1 peptide with HSA, MALDI-TOF-MS was used to compare the average molecular weight change between HSA and AT1-HSA. The mass-to-charge ratio
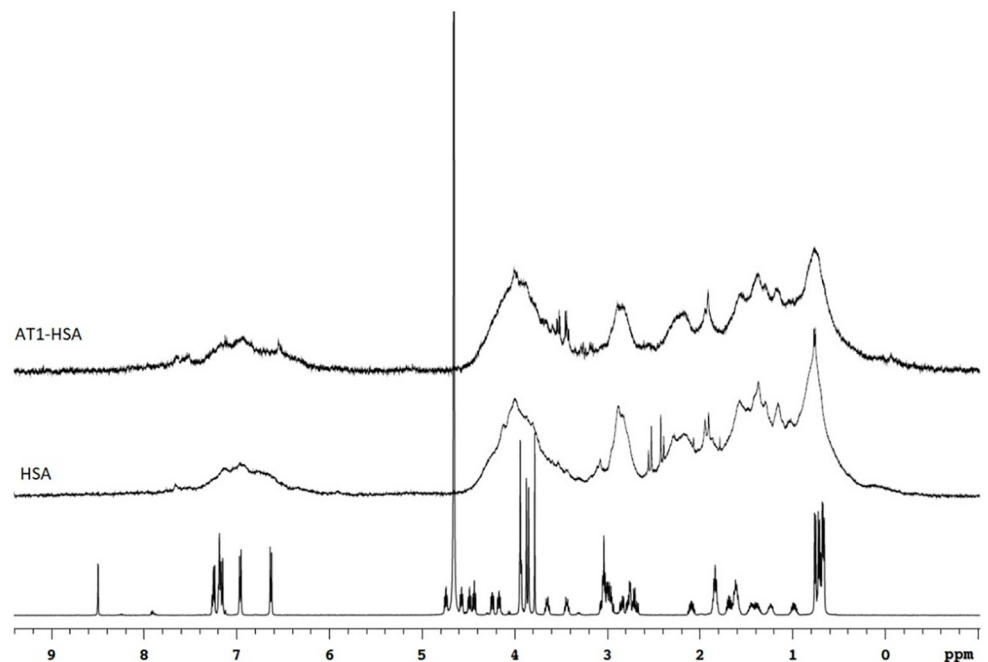
Fig 2. NMR analysis. 1H NMR based characterization of AT1-HSA, HSA and AT1 peptide. The AT1 peptide exhibits a spectrum with sharp peaks at δ = 0.5–1.0, δ = 1.1–2.1, δ = 2.8–3.8, δ = 4.0–5.0 and δ = 6.3–7.3. The peaks at δ = 6.8 due to tyrosine and around δ = 3.8–4.0 due to glycine from the AT1 peptide can be seen on the AT1-HSA spectrum around δ = 3.5–4.0 and 6.8 ppm.
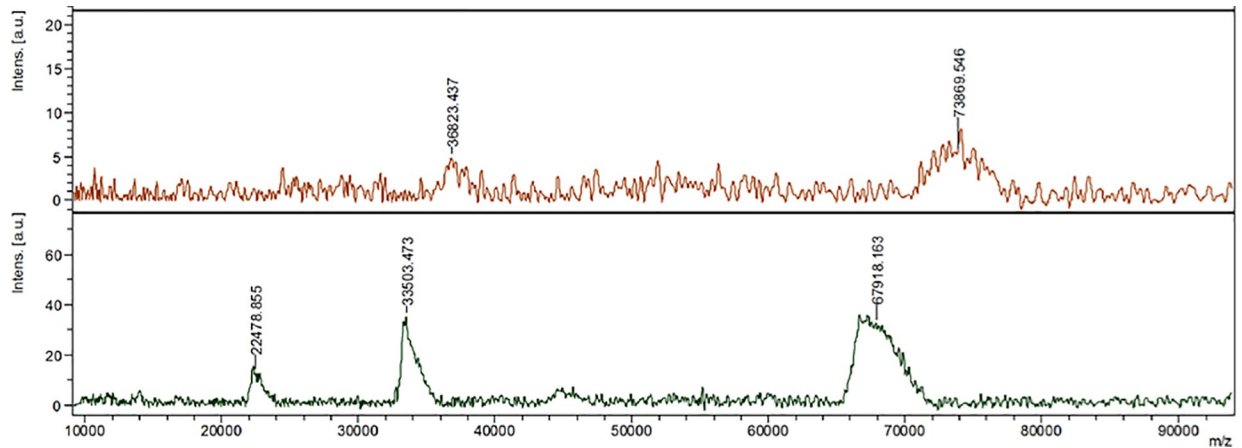
**Fig 3. Mass spectrometry analysis.** HSA (lower) and AT1-HSA (upper) was analyzed by Matrix-Assisted Laser Desorption/Ionization Time of Flight Mass Spectrometry. The m/z ratio of the AT1-HSA peak was at least 7000 higher than that of the HSA peak, which demonstrated that AT1 was successfully conjugated to the surface of HSA.

https://doi.org/10.1371/journal.pone.0254305.g003

(m/z) of the green peak (AT1-HSA) was approximately 7000 higher than the red peak (HSA). The molecular weights of the AT1 peptide, 5(6)-Carboxyfluorescein-NHS, EDC and Sulfo-NHS is 1274, 376.32, 190 and 217 g/mol, respectively. Upon calculating the cumulative molecular weight of AT1-HSA, and comparing with HSA protein, it can be inferred that at least 3 molecules of AT1 were successfully conjugated with the surface of each HSA molecule (**Fig 3**).

Nanoparticle characterization

The nanoparticles size was determined using DLS and laser Doppler anemometry for zeta potential analysis. The particle size of AT1-HSA-MRN-NPs was 215.2±4.7 nm with a zeta potential of -28.8±2.7 mV, and size of MRN-HSA-NPs (without AT1) was 189.6±3.8 nm with zeta potential of -27.5±4.6 mV. The morphology of the nanoparticles as observed using TEM under 13500X (**Fig 4(A))** and 55,000X magnification exhibited a near spherical shape with
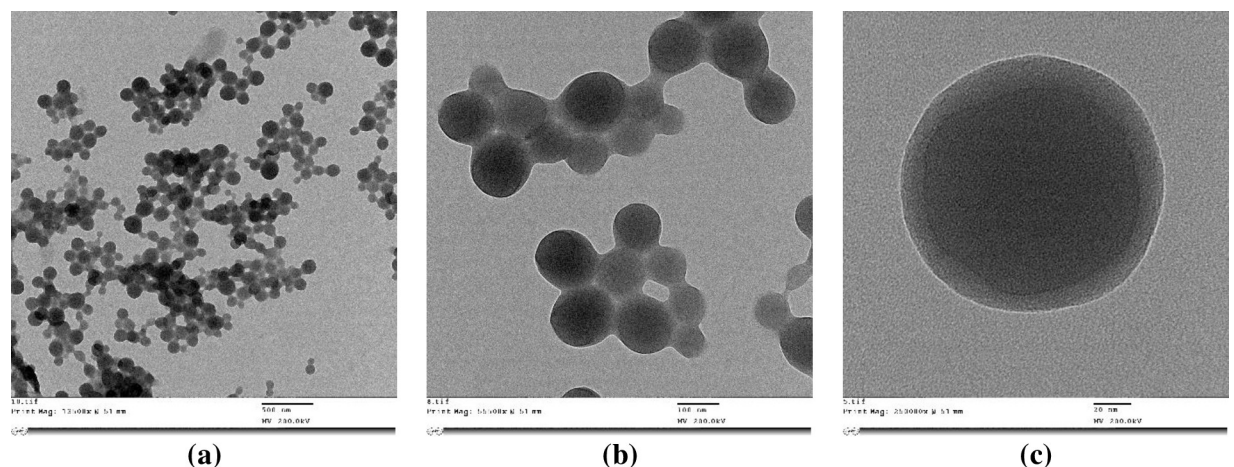
Fig 4. Nanoparticle morphology & size. Nanoparticle surface characterization using TEM analysis (a) Under magnification of 13,500X, AT1-HSA-MRN-NPs of size 215.2±4.7 nm and zeta potential of -28.8±2.7 mV (Scale = 500 nm) (b) Under magnification of 55,000X, AT1-HSA-MRN-NPs with moderately uniform particle size (Scale = 100 nm); (c) Under 250,000X magnification, the AT1-HSA-MRN-NPs display a dark core surrounded by a bright membrane, which confirmed the distinct peptide layer (Scale = 20 nm).

https://doi.org/10.1371/journal.pone.0254305.g004
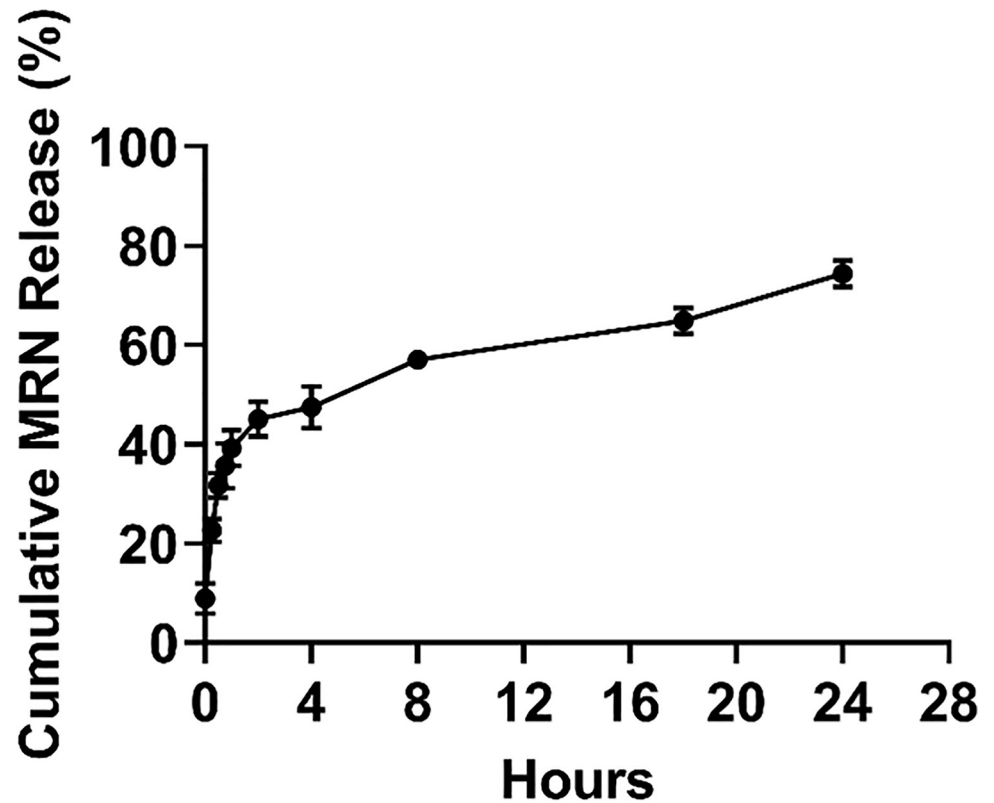
Fig 5. Cumulative drug release. Cumulative drug release (mean ± SD %, n = 3) of MRN from AT1-HSA-MRN-NPs with starting MRN concentration of 0.8 mg/mL over predetermined time intervals of 0, 0.25, 0.5, 0.75, 1, 2, 4, 8, 18 and 24 hrs.

https://doi.org/10.1371/journal.pone.0254305.g005

moderately uniform particle size and even distribution (**Fig 4(B)**). Under 250,000X magnification, the AT1-HSA-MRN-NPs had a dark core surrounded by a bright membrane, which confirmed the distinct layer (**Fig 4(C)**). The yield of the AT1-MRN-HSA-NPs was 75.6±2.5%, and encapsulation efficiency was 40.5±1.5%.

In Vitro drug release study

The drug release from AT1-HSA-MRN-NPs was studied by suspending 40 mg of nanoparticles in 10 mL PBS at 37°C and 120 rpm, with a starting MRN concentration of 0.8 mg/mL prepared from MRN/AT1-HSA (wt./wt.) ratio of 1:10. MRN showed a sustained release with approximately 50% of the MRN released between 4–6 hrs after which the release became slower with up to 75% of the MRN being released by 24 hrs (**Fig 5**). The drug released at various time points has been presented in Table 1.

Cell viability analysis

The MTT assay was performed for cell viability where H9c2 cells were treated with AT1-HSA-MRN-NPs, AT1-HSA-NPs, MRN-HSA-NPs and MRN Lactate containing 1mM MRN concentrations for 4, 24 and 48 hours. The 1mM MRN concentration was optimized in our previous study and is being used here for consistency of results [12, 35]. The safety analysis of MRN-HSA-NPs was conducted using HUVEC and H9c2 cells in our previous study and therefore was not repeated here [12, 35]. Results showed that the H9c2 cells treated with

Table 1. Cumulative drug release.

Time (hr)	% MRN Release
0	8.9 ± 3.1
0.25	22.6 ± 2.3
0.50	31.7 ± 2.5
0.75	35.6 ± 4.5
1	39.2 ± 3.6
2	45.1 ± 3.5
4	47.5 ± 4.2
8	57.1 ± 1.2
18	64.9 ± 2.6
24	74.4 ± 2.7

Cumulative release of MRN from AT1-HSA-MRN-NPs over 24 hours

[a]The results are presented as mean ± SD (n = 3).

https://doi.org/10.1371/journal.pone.0254305.t001

AT1-HSA-MRN-NPs, AT1-HSA-NPs and MRN Lactate for 4 hours showed cell viability of 73.4±1.4% (p = 0.0025), 101.7±2.9% (p = 0.9829) and 44.9±1.4% (p<0.0001) as compared to the control untreated cells, respectively (**Fig 6(A))**. Compared to the AT1-HSA-MRN-NPs, the cell viability of MRN-Lactate was significantly lower (p = 0.0016). At 24 hours, the cell viability was 55.5±3.7% (p = 0.0055), 70.8±11.2% (p = 0.0509) and 41.2±3.8% (p = 0.0009), respectively compared to the control group (**Fig 6(B))**, and at 48 hours, 52.4±2.1% (p = 0.0024), 65.9±11.2% (p = 0.0212) and 35.3±7.7% (p = 0.0001), respectively (**Fig 6(C))**. These results are also summarized in Table 2. Therefore, the AT1-HSA-MRN-NPs exhibit better safety characteristics and lesser cytotoxicity as compared to MRN Lactate. The *in vitro* cytotoxicity due to hypoxia and hypertrophy treatments was also investigated and compared with normal H9c2 cells. No significant difference in cell viability was observed between the 3 conditions (**Fig 7**).

Angiotensin II Type 1 receptor overexpression

The AT1R receptor overexpression was studied in hypoxic, hypertrophic and normal H9c2 cells. Results showed that hypoxic and hypertrophic cells exhibited a significantly higher
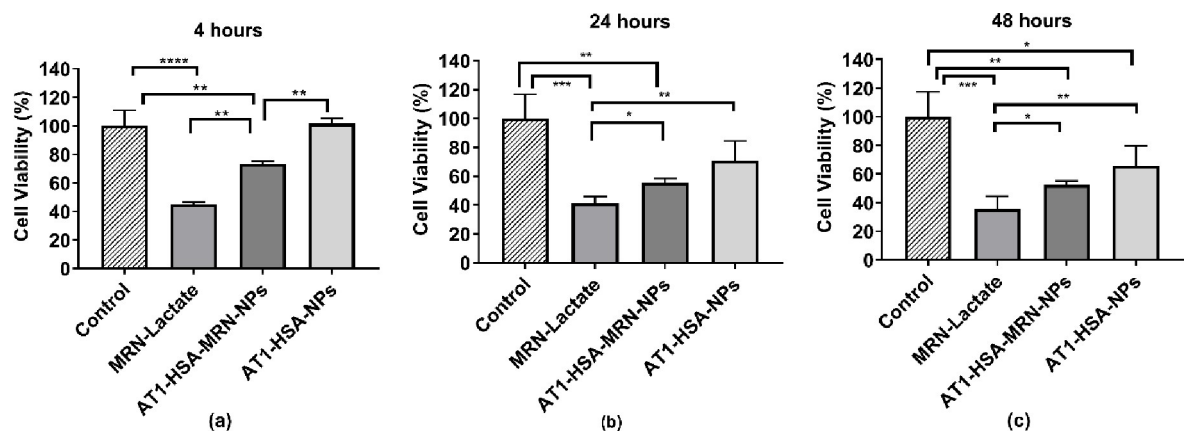
Fig 6. Cell viability analysis. Cell viability analysis on H9c2 cells treated with MRN-Lactate, AT1-HSA-MRN-NPs and AT1-HSA-NPs at 1 mM MRN concentration at (a) 4 hours, (b) 24 hours and (c) 48 hours. The graph shows a representative result of mean ± SD (n = 3). ****p<0.0001 was considered highly significant and ***p<0.001, **p<0.01 and *p<0.05 were considered significant based on Tukey's posthoc analysis.

https://doi.org/10.1371/journal.pone.0254305.g006

Table 2. H9c2 cell viability analysis.

Time point (hr)	Control (Untreated)	MRN Lactate	AT1-HSA-MRN-NPs	AT1-HSA-NPs
4	100 ± 8.9	44.9 ± 1.4	73.4 ± 1.4	101.7 ± 2.9
24	100 ± 13.7	41.2 ± 3.8	55.5 ± 3.7	70.8 ± 11.2
48	100 ± 15.1	35.3 ± 7.7	52.4 ± 2.1	65.9 ± 11.2

Percentage cell viability of H9c2 rat cardiomyoblasts post treatment with MRN-Lactate, AT1-HSA-MRN-NPs, and empty AT1-HSA-NPs at 4, 24 and 48 hrs.
[a]The results are presented as mean ± SD (n = 3).

expression of the AT1 receptors as compared to normal cells (p<0.0001). There was no significant differences between the hypoxic and hypertrophic conditions (p = 0.9883). The fluorescence intensity displayed by the hypoxic and hypertrophic cells was almost twice higher than that observed in the normal cells (**Fig 8**).

Intracellular nanoparticle uptake analysis

Since AT1 receptors are overexpressed on cardiomyocytes during HF, conjugating the nanoparticles with the AT1 peptide was anticipated to demonstrate higher uptake of the AT1-HSA-MRN-NPs through receptor-mediated endocytosis. The nanoparticle concentration was
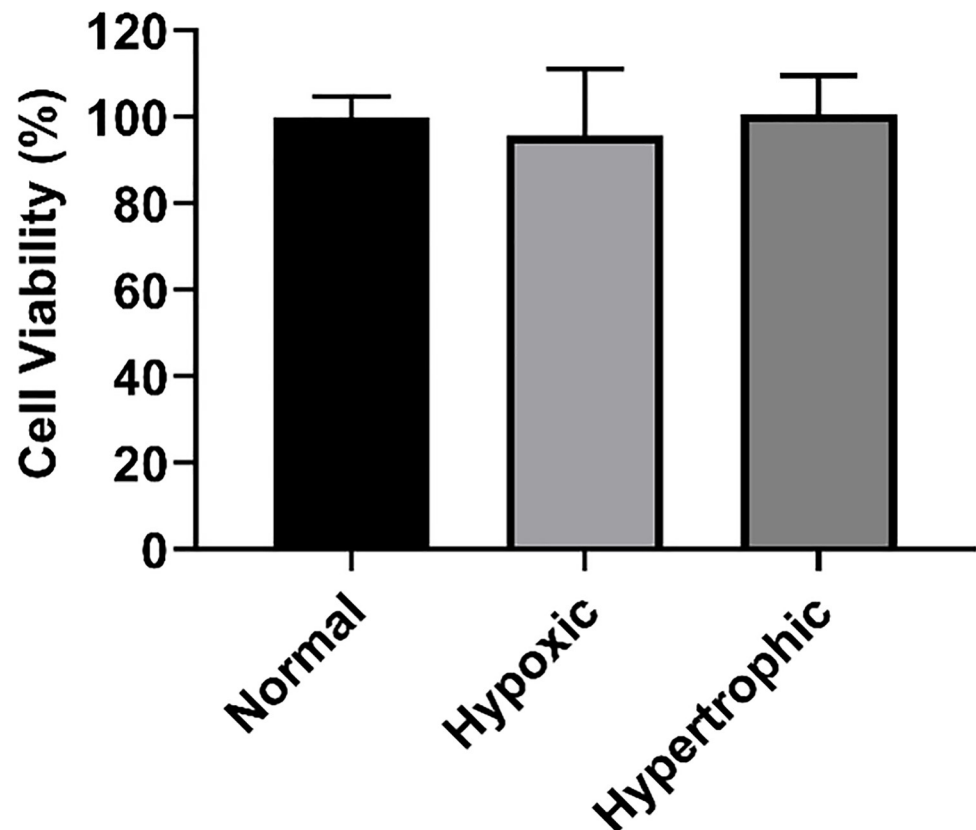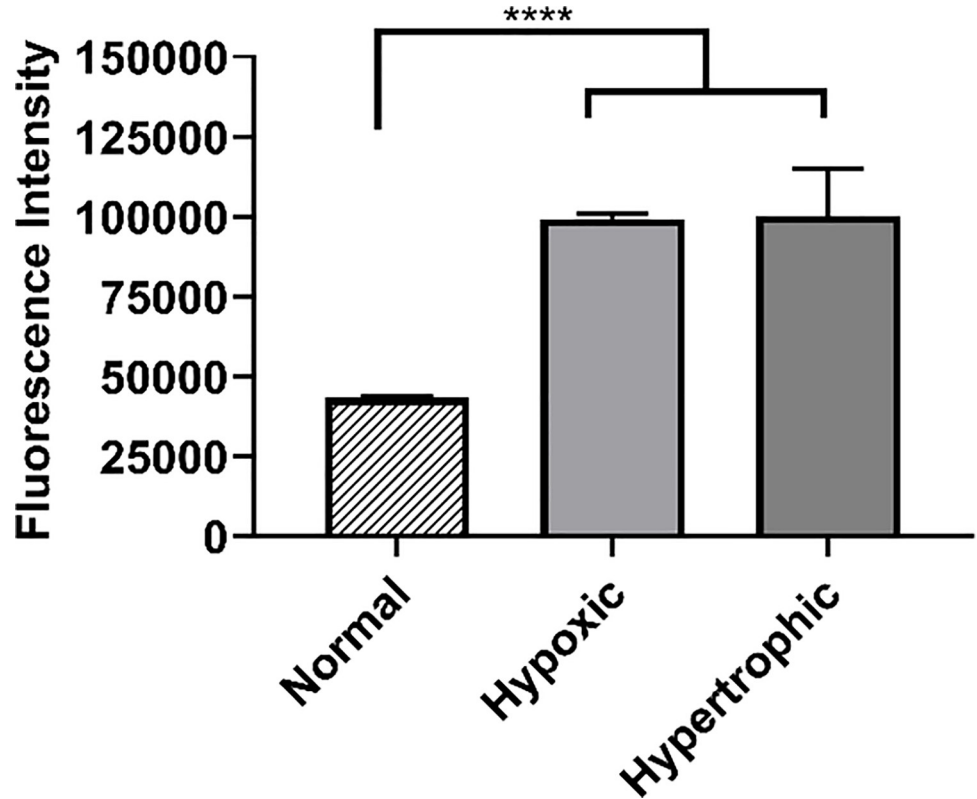

Fig 7. Effect of hypoxia & hypertrophy on cell viability. Viability of H9c2 cells treated for hypoxia and hypertrophy in comparison with normal cells (non-hypoxic and non-hypertrophic). There were no significant differences in cell viability amongst the groups.

Fig 8. Overexpression of AT1 receptor. AT1 expression in normal, hypoxic and hypertrophic H9c2 cells. Results are represented as mean ± SD (n = 3). ****p<0.0001 was considered highly significant based on Tukey's posthoc analysis.

https://doi.org/10.1371/journal.pone.0254305.g008

0.5 mg/mL. In normal (non-hypoxic, non-hypertrophic) cells, the AT1-HSA-MRN-NPs exhibited significantly higher fluorescence intensity as compared to the non-targeted MRN-HSA-NPs (p<0.001) and Scr-HSA-MRN-NPs (p<0.01, p = 0.0079) **(Fig 9(A))**. Similarly, in hypoxic cells, the AT1-HSA-MRN-NPs uptake was significantly higher (p<0.0001) than that of MRN-HSA-NPs and Scr-HSA-MRN-NPs (p = 0.0014) **(Fig 9(B))**. Also, for
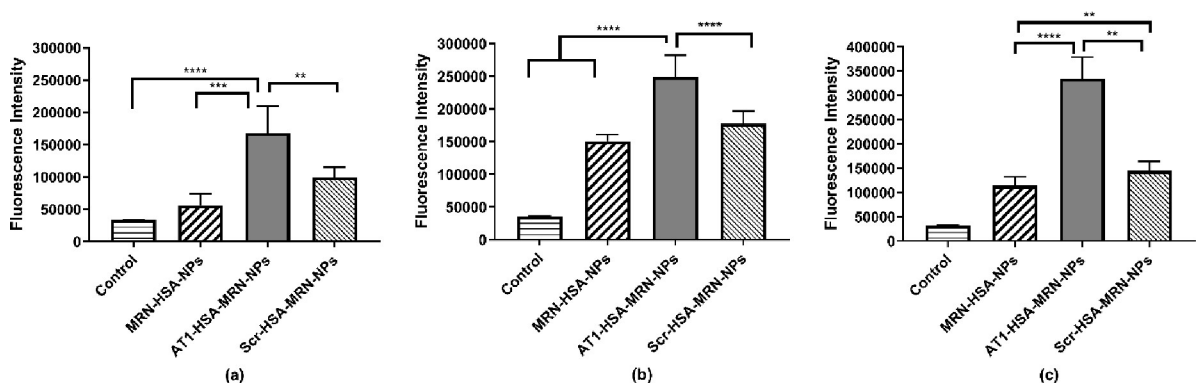
Fig 9. Intracellular uptake of nanoparticles. Intracellular uptake of MRN-HSA-NPs, AT1-HSA-MRN-NPs and Scr-HSA-MRN-NPs in H9c2 cells (a) Normal cells (non-hypoxic, non-hypertrophic), (b) Hypoxic cells and (c) Hypertrophic cells. The nanoparticle concentration was 0.5 mg/mL. The graph shows a representative result of mean ± SD (n = 3). ****p<0.0001 was considered highly significant and ***p<0.001, **p<0.01 were considered significant based on Tukey's posthoc analysis.

https://doi.org/10.1371/journal.pone.0254305.g009

hypertrophic cells, the uptake of AT1-HSA-MRN-NPs was significantly greater (p<0.0001) than that of MRN-HSA-NPs (p<0.0001) and Scr-HSA-MRN-NPs (p<0.0001) **(Fig 9(C))**.

Also, normal H9c2 cells exhibited significantly lesser uptake of AT1-HSA-MRN-NPs under hypoxia (p = 0.0163) and hypertrophy (p = 0.0015) There were no significant differences in the uptake of MRN-HSA-NPs (p = 0.0827) and Scr-HSA-MRN-NPs (p = 0.1954) under hypoxic and hypertrophic conditions either.

Discussion

The urgent need to effectively treat MI and HF has led to research and innovation of various new strategies and treatment modalities. These include delivery of drugs, growth factors, cytokines and other molecules for myocardial regeneration or treatment [36, 37]. However, due to inherent limitations with most treatment strategies such as lack of target specificity, low bioavailability, cardiac rejection while heart pumping, or non-specific distribution, the therapeutic effect is lessened [38]. The emerging studies on nanoparticles and targeted drug delivery systems have displayed promising results, however, their efficacy remains dependent on the drug binding capacity, solubility, nanoparticle degradability and plasma retention time [39]. In this study, keeping in view the intended features of ideal drug delivery systems, a targeted nanoparticle formulation was synthesized. The HSA surface was modified to attach a targeting ligand, AT1 peptide, to achieve superior delivery characteristics. The AT1 peptide shows specificity for the AT1 receptor present on the myocardium, which is found to be overexpressed under CHF conditions [6–8]. Using the AT1 peptide as the targeting moiety will facilitate receptor-mediated nanoparticle uptake. Though the angiotensin is a major axis in HF, used for drug-targeting by ACE inhibitors or angiotensin receptor blockers, we are yet to study the study the effect of AT1-HSA-MRN-NPs on receptor activity. However, the targeted delivery of MRN via AT1 receptor-mediated endocytosis of the nanoparticles is aimed at treating HF in an effective manner, thus suppressing exactly these potential effects [40]. The AT1 peptide was conjugated to the HSA surface through a two-step covalent chemical reaction. The 5(6)-Carboxyfluorescein-NHS targets primary amines such as in the side chain of lysine residues, to form stable amide bonds. This allows the carboxylic group to undergo a carbodiimide reaction with EDC, at pH 5.5, forming an unstable amine-reactive O-acylisourea intermediate. This unstable intermediate is further reacted with the Sulfo-NHS and the amine groups on AT1 peptide to release urea as a byproduct and form stable AT1-HSA. Literature suggests that the peptide (NH_2-Gly-Gly-Gly-Gly-Asp-Arg-Val-Tyr-Ile-His-Pro-Phe-NH_2) binds with the AT1 receptor over a sizeable binding transmembrane domain (TMD) through interactions between Asp1 (of peptide) with His183 in the second loop of the TMD, Arg2 of peptide with Asp281 in TMD-7, aromatic side chains of Phe8 of peptide with His256, Val254 and Phe259 of the domain, and Tyr4 of the peptide with Asn111 of TMD-3 [41, 42].

The pre-modification of the HSA by conjugation with the AT1 peptide was preferred over post-modification of the HSA-NPs as the latter may cause drug loss and leakage during the synthesis and purification. NMR and MALDI-TOF confirmed the binding of AT1 peptide to the HSA surface. In NMR results, HSA shows broad peaks owing to the high molecular weight of 66.5 kDa, whereas the AT1 peptide, with a molecular weight of ~ 1274 g/mol exhibits a clear spectrum showing chemical shifts due to the presence of the amino acid residues. Due to the large differences in molecular weights, the AT1-HSA spectrum resembles the HSA with visible differences at 6.8 and 4.0 ppm indicating AT1 binding. To confirm this, MALDI-TOF-MS was performed. The spectrum on the x-axis represents the m/z (mass/charge) ratio which was

73869.546 for AT1-HSA and 67918.163 for HSA, which was 7000 higher. Considering the mass of the AT1 peptide, the HSA and the cross-linkers, at least 3 AT1 peptide molecules were bound to the HSA surface.

The AT1-HSA-MRN-NPs were formed by the ethanol desolvation process [12, 30]. The nanoparticles exhibited a spherical structure as observed under TEM. The AT1-HSA-MRN-NP size was 215.2±4.7 nm with a zeta potential of -28.8±2.7 mV, in comparison with AT1-HSA-NPs with a size of 189.6±3.8 nm and zeta potential of -27.5±4.6 mV. Typically, particles less than 100 nm size undergo clearance by entering lymphatic capillaries, whereas particles in the size range of 250 nm—1μm are identified by macrophages and removed by the reticuloendothelial system [43, 44]. The chances of opsonization are also lowered with reduction in surface curvature. The nanoparticles prepared in this study were in the size range of 100–250 nm with a negative zeta potential, which suggests greater physical stability as nanoparticle aggregation is prevented due to presence of negative charges [45]. The particle size being less than 250 nm suggests a prolonged blood circulation time as the particles will not be rapidly removed through opsonization [46, 47]. MRN release over 24 hrs from the nanoparticles further confirmed drug binding to the AT1-HSA-MRN-NPs. The binding characterization of MRN with HSA has been studied extensively in our previous study and was therefore not repeated here [12, 35]. Though the release of milrinone has been extensively studied previously with attempts to extend the release over time, only slight improvements have been observed in this area [48, 49]. Hence, drug delivery vehicles are needed for effective delivery of MRN to improve the circulation time and rapid clearance from the body along with a targeted approach to further enhance the cardiac uptake and drug activity [40, 50].

The *in vitro* cytotoxicity was evaluated on H9c2 cells treated with MRN-Lactate, AT1-HSA-MRN-NPs and AT1-HSA-NPs. MRN is clinically administered as a lactate formulation intravenously to adult as well as pediatric patients for HF and associated cardiac conditions [51]. However, the use of MRN Lactate is linked with side effects such as palpitation, cardiac arrythmia and renal dysfunction [52]. This may be attributed to the non-targeted delivery of MRN Lactate and hence the need for a continuous infusion to meet the dosage requirements. Using the targeted nanoparticle formulation, synthesized in this study, as drug carriers this limitation would be overcome, given their higher biocompatibility, higher retention time, drug binding capacity and characteristics of controlled drug release [53]. The cell viability of H9c2 cells was investigated at 4, 24 and 48 hours, with MRN Lactate exhibiting higher cytotoxicity as compared to AT1-HSA-MRN-NPs and AT1-HSA-NPs. The toxicity of the nanoparticles, both HSA-FITC-NPs as well as AT1-HSA-MRN-NPs without fluorescent tagging, has been studied in our previous studies, both *in vitro* as well as *in vivo* [12, 40]. It was found that the nanoparticles were non-toxic and safe to use in animals and with further testing, will show immense potential for patients. Evaluating nanoparticle toxicity is essential to ensure their suitability for use in future pre-clinical and clinical studies.

The intracellular uptake of the nanoparticles was investigated in normal (non-hypoxic, non-hypertrophic), hypoxic and hypertrophic H9c2 cells and H9c2 cells have been found to be more suitable for cardiac ischemia studies [54]. Inducing hypoxia and hypertrophy in cells closely mimics MI and HF conditions [34, 55, 56]. The cell viability analysis comparing the normal cell viability with that of hypoxic and hypertrophic H9c2 cells suggested that the hypoxia and hypertrophy inducing treatments were safe and did not cause cytotoxicity. Literature has widely suggested that under HF, the AT1 receptors present on the cardiomyocytes are overexpressed and these receptors could be blocked to reverse cardiac remodeling [7, 8]. Therefore, targeting the overexpressed AT1 receptors with the targeted AT1-HSA-MRN-NPs to hypoxic and hypertrophic cardiac cells allowed higher uptake of the AT1-HSA-MRN-NPs as compared to the non-targeted MRN-HSA-NPs and Scr-HSA-MRN-NPs. The Scr peptide-

tagged nanoparticles were used as a negative control to ensure that the higher uptake of AT1-HSA-MRN-NPs was a direct result of AT1 peptide mediated targeting and not passive uptake [5]. Also, the uptake of the AT1-HSA-MRN-NPs was significantly higher in hypoxic and hypertrophic cells vs the normal cells. These studies confirm the targeting ability of the AT1 peptide under MI and HF conditions and demonstrate that AT1-HSA-MRN-NPs can safely be used *in vivo* as targeted drug delivery systems for congestive heart failure and related conditions. In our future studies, we intend to perform *in vivo* testing using fluorescence imaging to assess the uptake and activity on the drug payload. These studies will include pharmacokinetics, biodistribution and measurement of cardiac function along with toxicity analysis.

Conclusion

To summarize, we have synthesized and developed stable AT1 peptide conjugated albumin nanoparticles to deliver MRN in a targeted manner for heart failure treatment. This novel drug delivery system demonstrates physical stability, release, biocompatibility, specific targeting ability and higher cellular uptake. Also, as compared to the non-targeted MRN Lactate, AT1-HSA-MRN-NPs show greater biocompatibility in cardiomyoblasts. In future, the performance of AT1-HSA-MRN-NPs will be evaluated in a rat model of CHF along with MRN pharmacokinetics. This targeted therapy is anticipated to be more effective in improve the cardiac function in CHF as compared to the currently available treatments.

Acknowledgments

Author Contributions

Conceptualization: Nikita Lomis, Dominique Shum-Tim.

Data curation: Nikita Lomis, Susan Westfall, Dominique Shum-Tim.

Formal analysis: Nikita Lomis.

Funding acquisition: Satya Prakash.

Investigation: Nikita Lomis, Satya Prakash.

Methodology: Nikita Lomis, Susan Westfall.

Project administration: Satya Prakash.

Resources: Satya Prakash.

Software: Nikita Lomis.

Supervision: Satya Prakash.

Validation: Nikita Lomis.

Visualization: Nikita Lomis.

Writing – original draft: Nikita Lomis.

Writing – review & editing: Nikita Lomis, Satya Prakash.

References

1. Benjamin E.J., et al., Heart disease and stroke statistics—2018 update: a report from the American Heart Association. Circulation, 2018. 137(12): p. e67–e492. https://doi.org/10.1161/CIR.0000000000000558 PMID: 29386200

2. Inamdar A.A. and Inamdar A.C., Heart Failure: Diagnosis, Management and Utilization. Journal of clinical medicine, 2016. 5(7): p. 62. https://doi.org/10.3390/jcm5070062 PMID: 27367736

3. Doenst T., et al., PCI and CABG for Treating Stable Coronary Artery Disease: JACC Review Topic of the Week. Journal of the American College of Cardiology, 2019. 73(8): p. 964–976. https://doi.org/10.1016/j.jacc.2018.11.053 PMID: 30819365

4. Taylor C.J., et al., Survival following a diagnosis of heart failure in primary care. Family practice, 2017. 34(2): p. 161–168. https://doi.org/10.1093/fampra/cmw145 PMID: 28137979

5. Dvir T., et al., Nanoparticles targeting the infarcted heart. Nano letters, 2011. 11(10): p. 4411–4414. https://doi.org/10.1021/nl2025882 PMID: 21899318

6. Rivard K., et al., Overexpression of type I angiotensin II receptors impairs excitation-contraction coupling in the mouse heart. American Journal of Physiology-Heart and Circulatory Physiology, 2011. https://doi.org/10.1152/ajpheart.01092.2010 PMID: 21856918

7. Paradis P., et al., Overexpression of angiotensin II type I receptor in cardiomyocytes induces cardiac hypertrophy and remodeling. Proceedings of the National Academy of Sciences of the United States of America, 2000. 97(2): p. 931–936. https://doi.org/10.1073/pnas.97.2.931 PMID: 10639182

8. Xu J., et al., Role of cardiac overexpression of angiotensin II in the regulation of cardiac function and remodeling post-myocardial infarction. American Journal of Physiology-Heart and Circulatory Physiology, 2007.

9. Tai C., et al., Effect of angiotensin-converting enzyme inhibitors and angiotensin II receptor blockers on cardiovascular events in patients with heart failure: a meta-analysis of randomized controlled trials. BMC cardiovascular disorders, 2017. 17(1): p. 257–257. https://doi.org/10.1186/s12872-017-0686-z PMID: 28982370

10. Khan M.S., et al., Dose of angiotensin-converting enzyme inhibitors and angiotensin receptor blockers and outcomes in heart failure: a meta-analysis. Circulation: Heart Failure, 2017. 10(8): p. e003956. https://doi.org/10.1161/CIRCHEARTFAILURE.117.003956 PMID: 28790052

11. Hennig R., et al., Multivalent targeting of AT1 receptors with angiotensin II-functionalized nanoparticles. J Drug Target, 2015. 23(7–8): p. 681–9. https://doi.org/10.3109/1061186X.2015.1035276 PMID: 25950599

12. Lomis N., et al., Novel Milrinone Nanoformulation for Use in Cardiovascular Diseases: Preparation and in Vitro Characterization. Molecular pharmaceutics, 2017. 15(7): p. 2489–2502.

13. Feneck R., Phosphodiesterase inhibitors and the cardiovascular system. Continuing Education in Anaesthesia, Critical Care & Pain, 2007. 7(6): p. 203–207.

14. Alousi A. and Johnson D., Pharmacology of the bipyridines: amrinone and milrinone. Circulation, 1986. 73(3 Pt 2): p. III10–24. PMID: 2417744

15. Baim D.S., et al., Evaluation of a new bipyridine inotropic agent—milrinone—in patients with severe congestive heart failure. New England journal of medicine, 1983. 309(13): p. 748–756. https://doi.org/10.1056/NEJM198309293091302 PMID: 6888453

16. Barton P., et al., Hemodynamic effects of iv milrinone lactate in pediatric patients with septic shock: A prospective, double-blinded, randomized, placebo-controlled, interventional study. CHEST Journal, 1996. 109(5): p. 1302–1312.

17. Wang Z., et al., Combination therapy with milrinone and esmolol for heart protection in patients with severe sepsis: a prospective, randomized trial. Clinical drug investigation, 2015. 35(11): p. 707–716. https://doi.org/10.1007/s40261-015-0325-3 PMID: 26387030

18. de Boer R.A. and van Veldhuisen D.J., ACE-inhibitors, Beta-blockers or the Combination in Heart Failure: Is It Just an A–B–C? Cardiovascular Drugs and Therapy, 2008. 22(4): p. 261–263. https://doi.org/10.1007/s10557-008-6107-x PMID: 18418705

19. Cuffe M.S., et al., Short-term intravenous milrinone for acute exacerbation of chronic heart failure: a randomized controlled trial. Jama, 2002. 287(12): p. 1541–1547. https://doi.org/10.1001/jama.287.12.1541 PMID: 11911756

20. Abbasi S., et al., Cationic albumin nanoparticles for enhanced drug delivery to treat breast cancer: preparation and in vitro assessment. Journal of drug delivery, 2011. 2012. https://doi.org/10.1155/2012/686108 PMID: 22187654

21. Sebak S., et al., Human serum albumin nanoparticles as an efficient noscapine drug delivery system for potential use in breast cancer: preparation and in vitro analysis. International journal of nanomedicine, 2010. 5: p. 525. https://doi.org/10.2147/ijn.s10443 PMID: 20957217

22. Lomis N., et al., Human Serum Albumin Nanoparticles for Use in Cancer Drug Delivery: Process Optimization and In Vitro Characterization. Nanomaterials, 2016. 6(6): p. 116. https://doi.org/10.3390/nano6060116 PMID: 28335244

23. Lomis N., et al., Novel Milrinone Nanoformulation for Use in Cardiovascular Diseases: Preparation and in Vitro Characterization. Mol Pharm, 2018. 15(7): p. 2489–2502. https://doi.org/10.1021/acs.molpharmaceut.7b00360 PMID: 28837343

24. Jithan A., et al., Preparation and characterization of albumin nanoparticles encapsulating curcumin intended for the treatment of breast cancer. International journal of pharmaceutical investigation, 2011. 1(2): p. 119. https://doi.org/10.4103/2230-973X.82432 PMID: 23071931

25. Yu H., et al., A new bioavailability enhancement strategy of curcumin via self-assembly nano-complexation of curcumin and bovine serum albumin. Materials Science and Engineering: C, 2017. 75: p. 25–33. https://doi.org/10.1016/j.msec.2017.02.018 PMID: 28415461

26. Ji S., et al., RGD-conjugated albumin nanoparticles as a novel delivery vehicle in pancreatic cancer therapy. Cancer biology & therapy, 2012. 13(4): p. 206–215. https://doi.org/10.4161/cbt.13.4.18692 PMID: 22354009

27. Yu X., et al., Enhanced tumor targeting of cRGD peptide-conjugated albumin nanoparticles in the BxPC-3 cell line. Scientific reports, 2016. 6: p. 31539. https://doi.org/10.1038/srep31539 PMID: 27515795

28. Look J., et al., Ligand-modified human serum albumin nanoparticles for enhanced gene delivery. Molecular pharmaceutics, 2015. 12(9): p. 3202–3213. https://doi.org/10.1021/acs.molpharmaceut.5b00153 PMID: 26218774

29. Ruan C., et al., Substance P-modified human serum albumin nanoparticles loaded with paclitaxel for targeted therapy of glioma. Acta Pharmaceutica Sinica B, 2018. 8(1): p. 85–96. https://doi.org/10.1016/j.apsb.2017.09.008 PMID: 29872625

30. Langer K., et al., Optimization of the preparation process for human serum albumin (HSA) nanoparticles. International Journal of Pharmaceutics, 2003. 257(1): p. 169–180. https://doi.org/10.1016/s0378-5173(03)00134-0 PMID: 12711172

31. Langer K., et al., Human serum albumin (HSA) nanoparticles: reproducibility of preparation process and kinetics of enzymatic degradation. International journal of pharmaceutics, 2008. 347(1): p. 109–117. https://doi.org/10.1016/j.ijpharm.2007.06.028 PMID: 17681686

32. Siddiqui M., et al., Application of DDQ and p-chloranilic acid for the spectrophotometric estimation of milrinone in pharmaceutical formulations. Asian J Sci Res, 2009. 2: p. 135–145.

33. Wu D. and Yotnda P., Induction and testing of hypoxia in cell culture. Journal of visualized experiments: JoVE, 2011(54). https://doi.org/10.3791/2899 PMID: 21860378

34. Song R., et al., H2O2 induces myocardial hypertrophy in H9c2 cells: a potential role of Ube3a. Cardiovascular toxicology, 2015. 15(1): p. 23–28. https://doi.org/10.1007/s12012-014-9264-0 PMID: 24917194

35. Lomis N., et al., A novel milrinone nanoformulation for use in cardiovascular diseases: preparation and in vitro characterization. Mol Pharm, 2017.

36. Rebouças J.d.S., Santos-Magalhães N.S., and Formiga F.R., Cardiac regeneration using growth factors: advances and challenges. Arquivos brasileiros de cardiologia, 2016. 107(3): p. 271–275. https://doi.org/10.5935/abc.20160097 PMID: 27355588

37. Tang Y., et al., Targeted delivery of vascular endothelial growth factor improves stem cell therapy in a rat myocardial infarction model. Nanomedicine: Nanotechnology, Biology and Medicine, 2014. 10(8): p. 1711–1718.

38. Feric N.T. and Radisic M., Strategies and challenges to myocardial replacement therapy. Stem cells translational medicine, 2016. 5(4): p. 410–416. https://doi.org/10.5966/sctm.2015-0288 PMID: 26933042

39. Mudshinge S.R., et al., Nanoparticles: emerging carriers for drug delivery. Saudi pharmaceutical journal, 2011. 19(3): p. 129–141. https://doi.org/10.1016/j.jsps.2011.04.001 PMID: 23960751

40. Lomis N., et al., Albumin Nanoparticle Formulation for Heart-Targeted Drug Delivery: In Vivo Assessment of Congestive Heart Failure. Pharmaceuticals, 2021. 14(7): p. 697. https://doi.org/10.3390/ph14070697 PMID: 34358122

41. Guo D.F., et al., The angiotensin II type 1 receptor and receptor-associated proteins. Cell Research, 2001. 11(3): p. 165–180. https://doi.org/10.1038/sj.cr.7290083 PMID: 11642401

42. Clayton D., et al., Structural determinants for binding to angiotensin converting enzyme 2 (ACE2) and angiotensin receptors 1 and 2. Front Pharmacol, 2015. 6: p. 5. https://doi.org/10.3389/fphar.2015.00005 PMID: 25688208

43. Longmire M., Choyke P.L., and Kobayashi H., Clearance properties of nano-sized particles and molecules as imaging agents: considerations and caveats. Nanomedicine (Lond), 2008. 3(5): p. 703–17. https://doi.org/10.2217/17435889.3.5.703 PMID: 18817471

44. Harashima H., et al., Enhanced hepatic uptake of liposomes through complement activation depending on the size of liposomes. Pharm Res, 1994. 11(3): p. 402–6. https://doi.org/10.1023/a:1018965121222 PMID: 8008707

45. Xiao K., et al., The effect of surface charge on in vivo biodistribution of PEG-oligocholic acid based micellar nanoparticles. Biomaterials, 2011. 32(13): p. 3435–3446. https://doi.org/10.1016/j.biomaterials.2011.01.021 PMID: 21295849

46. Aderem A. and Underhill D.M., Mechanisms of phagocytosis in macrophages. Annu Rev Immunol, 1999. 17: p. 593–623. https://doi.org/10.1146/annurev.immunol.17.1.593 PMID: 10358769

47. Owens D.E. III and Peppas N.A., Opsonization, biodistribution, and pharmacokinetics of polymeric nanoparticles. International journal of pharmaceutics, 2006. 307(1): p. 93–102. https://doi.org/10.1016/j.ijpharm.2005.10.010 PMID: 16303268

48. Nanayakkara S., et al., Extended-Release Oral Milrinone for the Treatment of Heart Failure With Preserved Ejection Fraction. J Am Heart Assoc, 2020. 9(13): p. e015026. https://doi.org/10.1161/JAHA.119.015026 PMID: 32552264

49. Silverman D.N., Houston B.A., and Tedford R.J., Old Drug, New Trick? Oral Milrinone for Heart Failure With Preserved Ejection Fraction. Journal of the American Heart Association, 2020. 9(13): p. e017170–e017170. https://doi.org/10.1161/JAHA.120.017170 PMID: 32552221

50. Al Kindi H., et al., Sustained release of milrinone delivered via microparticles in a rodent model of myocardial infarction. J Thorac Cardiovasc Surg, 2014. 148(5): p. 2316–23. https://doi.org/10.1016/j.jtcvs.2014.07.033 PMID: 25175952

51. Tang X., et al., Milrinone for the Treatment of Acute Heart Failure After Acute Myocardial Infarction: A Systematic Review and Meta-Analysis. Basic & clinical pharmacology & toxicology, 2015. 117(3): p. 186–194. https://doi.org/10.1111/bcpt.12385 PMID: 25625413

52. Stewart D. and McPherson M.L., Symptom management challenges in heart failure: pharmacotherapy considerations. Heart failure reviews, 2017. 22(5): p. 525–534. https://doi.org/10.1007/s10741-017-9632-5 PMID: 28646467

53. Loureiro A., et al., Albumin-based nanodevices as drug carriers. Current pharmaceutical design, 2016. 22(10): p. 1371–1390. https://doi.org/10.2174/1381612822666160125114900 PMID: 26806342

54. Kuznetsov A.V., et al., H9c2 and HL-1 cells demonstrate distinct features of energy metabolism, mitochondrial function and sensitivity to hypoxia-reoxygenation. Biochimica et Biophysica Acta (BBA)-Molecular Cell Research, 2015. 1853(2): p. 276–284. https://doi.org/10.1016/j.bbamcr.2014.11.015 PMID: 25450968

55. Dickhout J.G., Carlisle R.E., and Austin R.C., Interrelationship between cardiac hypertrophy, heart failure, and chronic kidney disease: endoplasmic reticulum stress as a mediator of pathogenesis. Circulation Research, 2011. 108(5): p. 629–642. https://doi.org/10.1161/CIRCRESAHA.110.226803 PMID: 21372294

56. Zhang Z., et al., Knockdown of MicroRNA-122 Protects H9c2 Cardiomyocytes from Hypoxia-Induced Apoptosis and Promotes Autophagy. Medical science monitor: international medical journal of experimental and clinical research, 2017. 23: p. 4284–4290. https://doi.org/10.12659/msm.902936 PMID: 28871076